Desalination and Water Treatment
www.deswater.com
doi: 10.5004/dwt.2021.27839

242 (2021) 283–292
December

Chitosan modifications for azo dyes removal from wastewaters: Methyl orange dye model

H.M. Ahmed, S. Aboulhadeed, R.E. Khalifa, A.M. Omer, T.M. Tamer, M.S. Mohy-Eldin*

Polymer Materials Research Department, Advanced Technologies and New Materials Research Institute, City of Scientific Research and Technological Applications (SRTA-City), New Borg El-Arab City, P.O. Box: 21934, Alexandria, Egypt, Tel. 002 034593414; emails: mmohyeldin@srtacity.sci.eg (M.S. Mohy-Eldin), malak.scientist@gmail.com (H.M. Ahmed), s.a.aboulhadeed@gmail.com (S. Aboulhadeed), randaghonim@gmail.com (R.E. Khalifa), amomar@srtacity.sci.eg (A.M. Omer), tmahmoud@srtacity.sci.eg (T.M. Tamer)

Received 21 May 2021; Accepted 25 September 2021

ABSTRACT

The objective of the present work is the synthesis and characterization of the newly formed chitosan Schiff base derivative for the removal of azo dye, using Methyl orange (MO) as a model from wastewater. The chitosan Schiff base derivative was developed by reaction of chitosan with 4-methoxybenzaldehyde to have chitosan Schiff base (Cs/MeB) in the presence of glutaraldehyde as a crosslinker. The structures were characterized using Fourier-transform infrared, thermal gravimetric analysis, scanning electron microscopy, and differential scanning calorimetry. A batch system was applied to study the adsorption of MO dye from aqueous solutions using the developed chitosan Schiff base (Cs/MeB) compared to pure cross-linked chitosan. Experiments were carried out as a function of contact time, initial dye concentration, system temperature, system pH, agitation rate and adsorbent dosage on dye removing percent (%).

Keywords: Chitosan; 4-methoxybenzaldehyde; Schiff base; Azo dye; Methyl orange; Adsorption

1. Introduction

A wide variant of pollutants can contaminate the water either individually or coordinately, such as heavy metals, dyes, and pharmaceutics wastes [1–3]. Different type of water-soluble dyes such as methylene blue has a wide industrial use [4] and cause very harmful impacts on the life quality [5]. The azo dyes have a dominant contribution in the textile industries and cause mainly health problems [6]. Accordingly, the contamination of the wastewater by such dyes is a high priority environmental challenge, and many techniques were developed to eliminate including; photodecomposition, ceramic ultrafiltration membrane, degradation by electrochemical oxidation techniques, biological combined anaerobic-aerobic treatment, and finally, the most widely used; adsorption technique [7–11].

Since cost is the significant factor for any process/technology to find eventual adoption in industries, an efficient and widely available cheaper substitutes-based method of dye removal/remediation would be highly desirable to address cost issues. At this point, the biopolymers-based materials for the removal of the dye come first. Dassanayake et al. [12] reviewed the recent advances in biopolymer-based dye removal technologies. The review highlights and presents a review of recent literature on the utilization of the most widely available biopolymers, specifically cellulose, chitin and chitosan-based products for dye removal. The focus has been limited to the three

* Corresponding author.

1944-3994/1944-3986 © 2021 Desalination Publications. All rights reserved.

most widely explored technologies: adsorption, advanced oxidation processes and membrane filtration. Due to their high efficiency in dye removal coupled with environmental benignity, scalability, low cost and non-toxicity, biopolymer-based dye removal technologies have the potential to become sustainable alternatives for the remediation of industrial dye effluents as well as contaminated water bodies.

Kyzas et al. [13] reviewed chitosan adsorbents for dye removal. The major advantage of chitosan is the existence of modifiable positions in its chemical structure. Modification of the chitosan molecule by (i) grafting (inserting functional groups) or (ii) crosslinking reactions (uniting the macromolecular chains with each other) leads to the formation of chitosan derivatives with superior properties (enhancement of adsorption capacity and resistance in extreme medium conditions, respectively).

Freire et al. [14] synthesized chitosan/magnetite nanoparticles (ChM) based on co-precipitation reaction under ultrasound (US) irradiation. The adsorption capacity for Methyl orange (MO) was found 70.85 mg/g.

Dong et al. [15] developed polyamine chitosan adsorbent, reach with extra amine groups on C6, for the enhanced adsorption of anionic dyes (Congo red and Methyl orange) from water. The developed polyamine chitosan adsorbent shows significantly greater adsorption capacities (625 mg/g) compared with chitosan (71 mg/g) according to the monolayer Langmuir model. The increased adsorption performance was attributed to a large number of primary amine groups on the surfaces. The adsorption mechanism was based on electrostatic interaction, while the adsorption process was mainly physisorption.

Labidi et al. [16] grafted chitosan with acrylamide to have chitosan-graft-polyacrylamide for evaluation of its capacity in the removal of MO dye from water solution. The chitosan-graft-polyacrylamide removed 100% of MO from 1 ppm solution within 30 min.

Ahmad et al. [17] synthesized a novel chitosan-grafted polyorthoethylaniline biocomposite and tested the adsorption of MO dye. The Langmuir isotherm model adsorption capacity of 45.7mg/g was evaluated.

The modification of chitosan through click reaction with aldehydes to form Schiff bases has attracted much attention recently due to the ease of the modification in one step and the wide range of Schiff bases obtained with different hydrophobic-hydrophilic characters. The cheap cost of the naturally extracted aldehydes and so chitosan acquired the chitosan Schiff bases and advantage.

Alabbad [18] developed an efficient chitosan-iso-vanillin Schiff base polymer adsorbent and evaluated the removal of Methyl orange (MO) dye from wastewater. The monolayer Langmuir adsorption capacity reaches 666.6 mg/g.

Yuvaraja et al. [19] developed a novel, eco-friendly aminated chitosan-terephthalaldehyde Schiff's base-ZnO composite (ACSSB@ZnO) and utilized it to remove MO from aqueous environment. The highest sorption capacity of ACSSB@ZnOwas observed to be 111.11 mg/g at 323 K.

Huang et al. [20] prepared salicylaldehyde-chitosan Schiff base (SCSB), an electropositive adsorbent. The results showed that SCSB exhibited electrostatic adsorption on anionic dyes with a better adsorption performance than chitosan. The obtained adsorption capacity was found at 57.57 mg/g for MO dye.

In the continuation search to development of an efficient and widely available cheaper substitutes-based adsorbent materials of dye removal/remediation, since the cost is the significant factor for any process/technology to find eventual adoption in industries, the present study aimed to develop a novel chitosan-4-methoxybenzaldehyde Schiff base (Cs/MeB) for the removal of Methyl orange (MO) from wastewater as an azo-dye model, by click reaction of chitosan amine groups of the 4-methoxybenzaldehyde to have an adsorbent with higher hydrophobicity and less positive charges sites. The 4-methoxybenzaldehyde was selected based on containing its chemical structure of both benzene aromatic ring and methyl hydrophobic groups matched its counterpart in the MO structure, which expected to promote the hydrophobic-hydrophobic interaction. Both chitosan Schiff base (Cs/MeB) derivative and chitosan were crosslinked by glutaraldehyde to have additional Schiff base formation with three-dimensional structures. The physic-chemical properties of the developed adsorbents were characterized using Fourier-transform infrared (FT-IR), thermal gravimetric analysis (TGA), scanning electron microscopy (SEM), and differential scanning calorimetry (DSC).

Finally, the developed chitosan Schiff base (Cs/MeB) derivative was examined in a batch tank reactor to remove the MO dye from aqueous solutions and compared to crosslinked chitosan. The impact of operational conditions such as contact time, initial dye concentration, system temperature, system pH, agitation rate and adsorbent dosage on the MO dye removing percent (%) was investigated.

2. Materials and methods

2.1. Materials

Chitosan (molecular weight: 100,000–300,000) was obtained from ACROS Organics™ (USA). Acetic acid (99.8%), methyl orange, 4-methoxybenzaldehyde were all purchased from Sigma-Aldrich (Germany). Sulfuric acid 98%, sodium hydroxide, ethanol, and phenolphthalein were purchased from El-Nasr Pharmaceutical Co for Chemicals (Egypt).

2.2. Methods

2.2.1. Preparation of chitosan and chitosan Schiff base derivative hydrogels

Coupling of chitosan amine groups with aldehyde was done according to Soliman et al. method [21]. In detail, (1 g) of the chitosan was dissolved in 50 mL acetic acid solution (2%) at ambient temperature overnight. Filtration of chitosan solution was carried out using cheesecloth to remove undissolved chitosan. Then a 10 mL of absolute ethanol was added carefully to the chitosan solution, with continuous stirring to have a homogenous solution. 31 mmole of 4-methoxybenzaldehyde previously dissolved in 10 mL ethanol was added to the above solution. After that, the temperature was rose to 70°C; the reaction mixture was left to react under continuous stirring for 6 h. Then 5 mL of 10%

glutaraldehyde was added to the solution to have 0.66% glutaraldehyde final concentration, with continuous stirring at 70°C for an additional 1 h. The obtained gels were collected by filtration, washed several times with Ethanol to remove any unreacted halide or aldehyde, and finally dried at 60°C under reduced pressure. The unmodified chitosan hydrogel was prepared under the same conditions without the addition of the aldehyde. The dried chitosan and chitosan Schiff base (Cs/MeB) hydrogels were grinding well, and particles size between 125–250 μm was collected using gradual mechanical sieving for further use in the MO adsorption process. Chitosan Schiff base (Cs/MeB) hydrogel was characterized and evaluated comparing to chitosan hydrogel (Cs).

2.3. Characterization

2.3.1. Physicochemical characterization

2.3.1.1. Water uptake (%)

The water uptake behaviour of the prepared hydrogel was investigated using distilled water (pH 5.4). Accurately weighed amounts of hydrogels were immersed in water and allowed to swell for 24 h at 37°C. The swollen hydrogel was periodically separated, and the moisture adhered to the surface of hydrogel was removed by blotting them gently in between two filter papers, immediately followed by weighing. The swelling degree of samples was determined according to the following formula [22]:

$$\text{Water uptake}\left(\%\right)=\left[\frac{M_t-M_0}{M_0}\right]\times 100 \tag{1}$$

where M_t is the weight of the swollen hydrogel and M_0 is the initial dry weight.

2.3.1.2. Ion exchange capacity of the hydrogel

A known weight of chitosan or Schiff base hydrogels were added to the known volume of 0.1 M H_2SO_4 solution, and the mixture was kept under shaking for 3 h. The mixture was filtered, and an aliquot was titrated against a standard solution of sodium hydroxide. Similarly, control titration without the addition of chitosan was also run. From the difference in the volume of NaOH required for neutralization, the ionic capacity of chitosan samples was calculated using the following equation:

$$\text{Ion exchange capacity (meq/g)}=\frac{\left(V_2-V_1\right)A}{W} \tag{2}$$

where V_2 and V_1 are the volumes of NaOH required for complete neutralization of H_2SO_4 in the absence and presence of chitosan membrane, respectively, A is the normality of NaOH and W is the weight of sample taken for analysis [23].

2.3.1.3. Infrared spectrophotometric

Infrared spectra were performed with Fourier-transform infrared spectrophotometer (Shimadzu FTIR – 8400 S, Japan) to confirm modification and prove the structure of the developed hydrogels.

2.3.1.4. Thermal gravimetric analysis

Analysis by TGA of samples was carried out using a thermogravimetric analyzer (Shimadzu TGA-50, Japan) under nitrogen to evidence changes in structure as a result of the modification. Samples were measured their weight loss starting from room temperature to 600°C at a heating rate of 10°C/min.

2.3.1.5. Differential scanning calorimetry analysis

Differential scanning calorimetric analysis of chitosan and chitosan Schiff base samples (~5 mg in sealed Al-pan) was carried out using Differential Scanning Calorimeter device (Shimadzu DSC-60A, Japan) in the temperature range of ambient to 350°C at a heating rate of 10°C/min under nitrogen flow (30 mL/min).

2.3.1.6. Scanning electron microscopic analysis

Samples were coated under a vacuum with a thin layer of gold before being examined by scanning electron microscopy. Morphological changes of the surface of the sample were followed using a secondary electron detector of SEM (Joel JSM 6360LA), Japan.

2.3.1.7. Batch equilibrium studies

The stock solution of 1 g/L of Methyl orange (MO) dye (1,000 ppm) was prepared by dissolving the appropriate amount of dye in distilled water then the used concentrations were obtained by dilution. All the adsorption experiments were conducted in 100 mL flasks by adding a given amount of adsorbent to 25 mL dye solution of different dye concentrations with different pH values and shaking in an orbital shaker for a given time. The adsorbate concentrations in the initial and final aqueous solutions were measured by using UV-Vis spectrophotometer at 465 nm. The amount of dye adsorbed was calculated from the difference between the initial concentration and the equilibrium one. The values of percentage removal were calculated using the following relationship:

$$\text{Dye removal}\left(\%\right)=\frac{\left(C_0-C_e\right)}{C_0}\times 100 \tag{3}$$

where C_0 is the initial dye concentration and C_e is the final dye concentration in supernatant.

3. Results and discussions

In the current research, new chitosan Schiff base (Cs/MeB) derivative hydrogel was prepared via coupling chitosan amine groups with 4-methoxybenzaldehyde followed by crosslinking with glutaraldehyde (Fig. 1). The prepared hydrogel was characterized using different characterization tools. The obtained hydrogel was evaluated as a

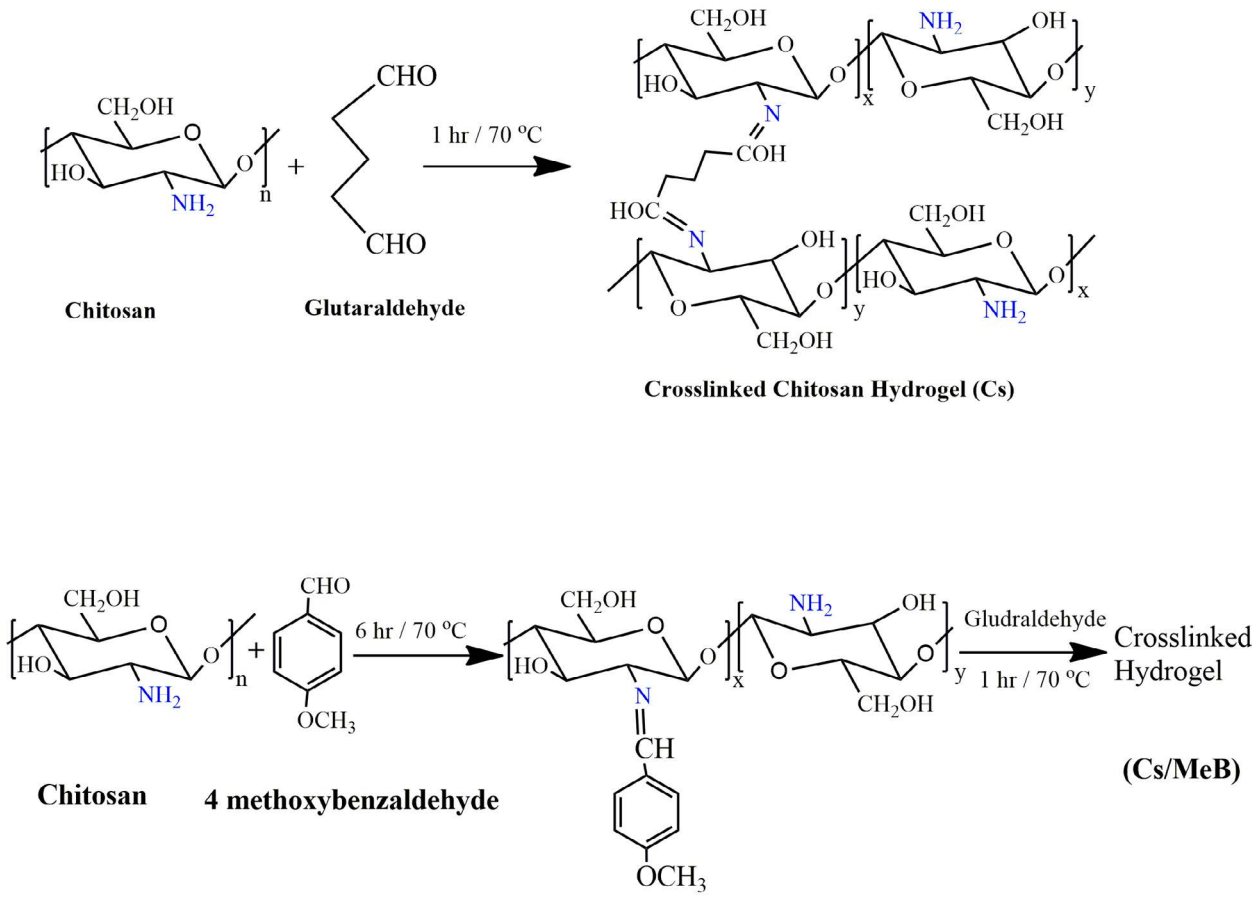

Fig. 1. Schematic preparation of chitosan and Cs/MeB hydrogels.

dye removal material using Methyl orange as a model for anionic dye.

3.1. Characterization

3.1.1. Physicochemical characterization

The cationic ion exchange capacity of chitosan and chitosan Schiff base (Cs/MeB) derivative demonstrate a decrease in free amine groups of chitosan hydrogel. The decrease of the ion exchange capacity of the chitosan from 4.48 to 2.84 meq/g of Cs/MeB can be explained by the consumption of amine groups in the reaction with 4-methoxybenzaldehyde. The decrease of the water uptake values of the prepared hydrogel from 213% (chitosan) to 130% (Cs/MeB) confirmed the consumption of amine groups in the reaction with 4-methoxybenzaldehyde.

3.1.2. Fourier-transform infrared spectroscopy

Function groups of chitosan and chitosan Schiff base (Cs/MeB) hydrogels were estimated using FT-IR. Fig. 2 illustrates the polysaccharide function groups included hydroxyl at 3,200–3,600 cm^{-1}, aliphatic C–H bond at 2,850–1,960 cm^{-1} and C=O, C–O–C and C–O at 1,637, 1,157 and 1,025 cm^{-1}, respectively. On the other hand, coupling

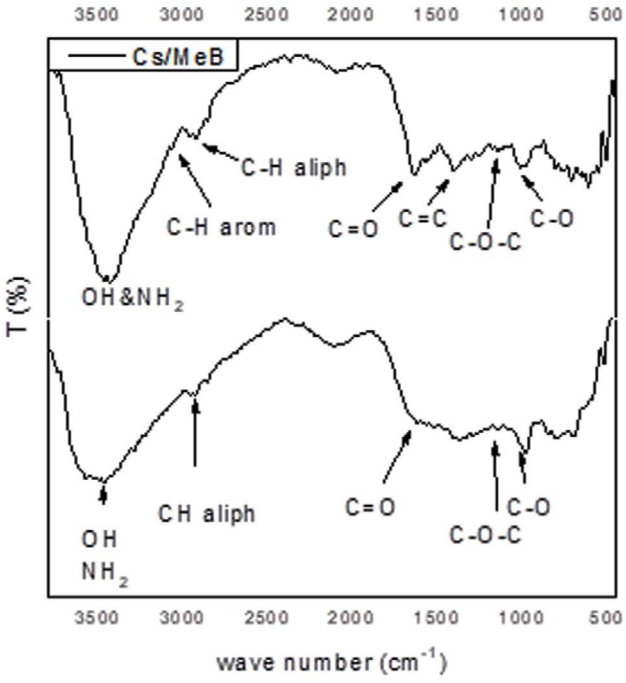

Fig. 2. FT-IR of Cs and Cs/MeB hydrogels.

chitosan with 4-methoxybenzaldehyde generates another type of peaks such as aromatic C–H at 3,066 cm^{-1} and C=C at 1,421 cm^{-1} [24–26].

3.1.3. Thermal gravimetric analysis

Thermal degradation of chitosan and its derivatives hydrogel was investigated from 25°C–600°C and presented in Fig. 3. Moisture loss at the initial degradation step ~100°C of chitosan and (Cs/MeB) are 6.77% and 7.97%, respectively. The second degradation step was started at 220°C that corresponding to the thermal decomposition of glucose pyranose ring to form crosslinked residue [27]. Slightly higher degradation of Cs/MeB than chitosan was observed indicates a neglected impact of the Schiff base formation on the thermal stability [28].

3.1.4. Differential scanning calorimetry

Fig. 4 displays the DSC chart of chitosan hydrogel and chitosan Schiff base (Cs/MeB) derivative. The endothermic peak below 100°C was associated with evaporation of piping water that was trapped by chains during preparation steps [29,30]. The next event was described as an exothermic peak between 220°C–320°C as a result of the destructive decomposition of the chitosan pyranose ring along the polymer backbone [31].

3.1.5. Scanning electron microscope

Fig. 5 represents the morphological structure of the chitosan and chitosan Schiff base (Cs/MeB) derivative hydrogels. Analyses of the pictures demonstrate an almost homogenous surface of the chitosan adsorbent (Fig. 5a). On the other side, morphological changes of the chitosan Schiff base (Cs/MeB) have been observed with the formation of new structures on the surface, flacks flowers like, which increase the outer surface area. In addition, new pores formation with different sizes, which provides an additional internal pores surface area, was recognized as indicated in Fig. 5b. This phenomenon can be described by the presence of heterogeneous groups labelled on the repeating polysaccharide, which distorts the internal order of chains and creating new-formed structures and pores, which consequently increases the external and internal surface area [26].

3.2. Adsorption process

In this work, we investigated the sorption behaviour of chitosan and chitosan Schiff base (Cs/MeB) derivative hydrogels, which give the maximum removal per cent, and its applicability to artificially contaminated water with Methyl orange (MO) solution.

A batch experiment was performed in which aqueous solutions of the MO were prepared. The adsorption behaviours of the hydrogels towards the MO were optimized under different adsorption conditions of time, temperature, dye pH, agitation rate, adsorbent dosage, and MO initial concentrations.

3.2.1. Effect of time

Fig. 6 presented the time profile of the MO adsorption process by Cs and Cs/MeB hydrogels. The adsorption at the initial stages is relatively rapid and then gradually decreases with the progress of adsorption until it reaches an equilibrium state. In the process of dye adsorption, initially, dye molecules have first to encounter the boundary layer effect, and then it has to diffuse from boundary layer film onto the adsorbent surface and then finally, it has to diffuse into the porous structure of the adsorbent [32]. The rapid adsorption at the initial contact time can be referring to the availability of the higher positively active sites along hydrogel surface and pores [33]. With the progress of the adsorption process, the dye removal rate going to slow down for many reasons, such as (a) reducing of the free adsorbing active sites on the adsorbents, (b) the repulsion interaction between the negative adsorbed dye molecules on the adsorbents, in the first stage, and the remaining free dye molecules in the solution, and (c) decreases of the dyes concentration gradients between the adsorbents solid phase and the dye solution phase which is the motivating force of the adsorption process. Many interesting

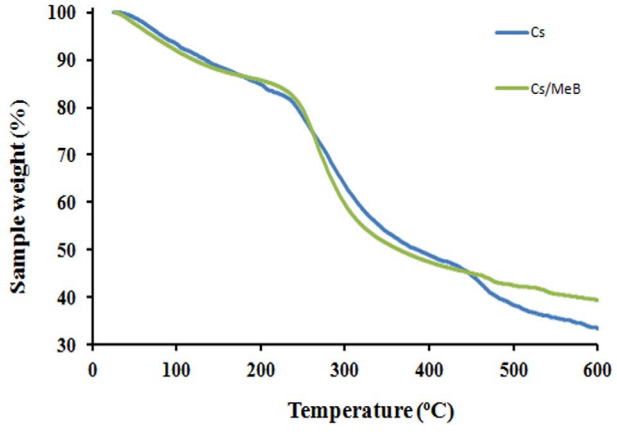

Fig. 3. TGA of Cs and Cs/MeB hydrogels.

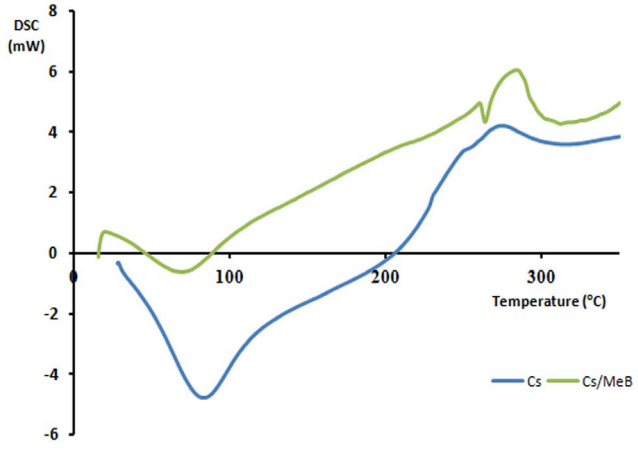

Fig. 4. DSC of Cs and Cs/MeB hydrogels.

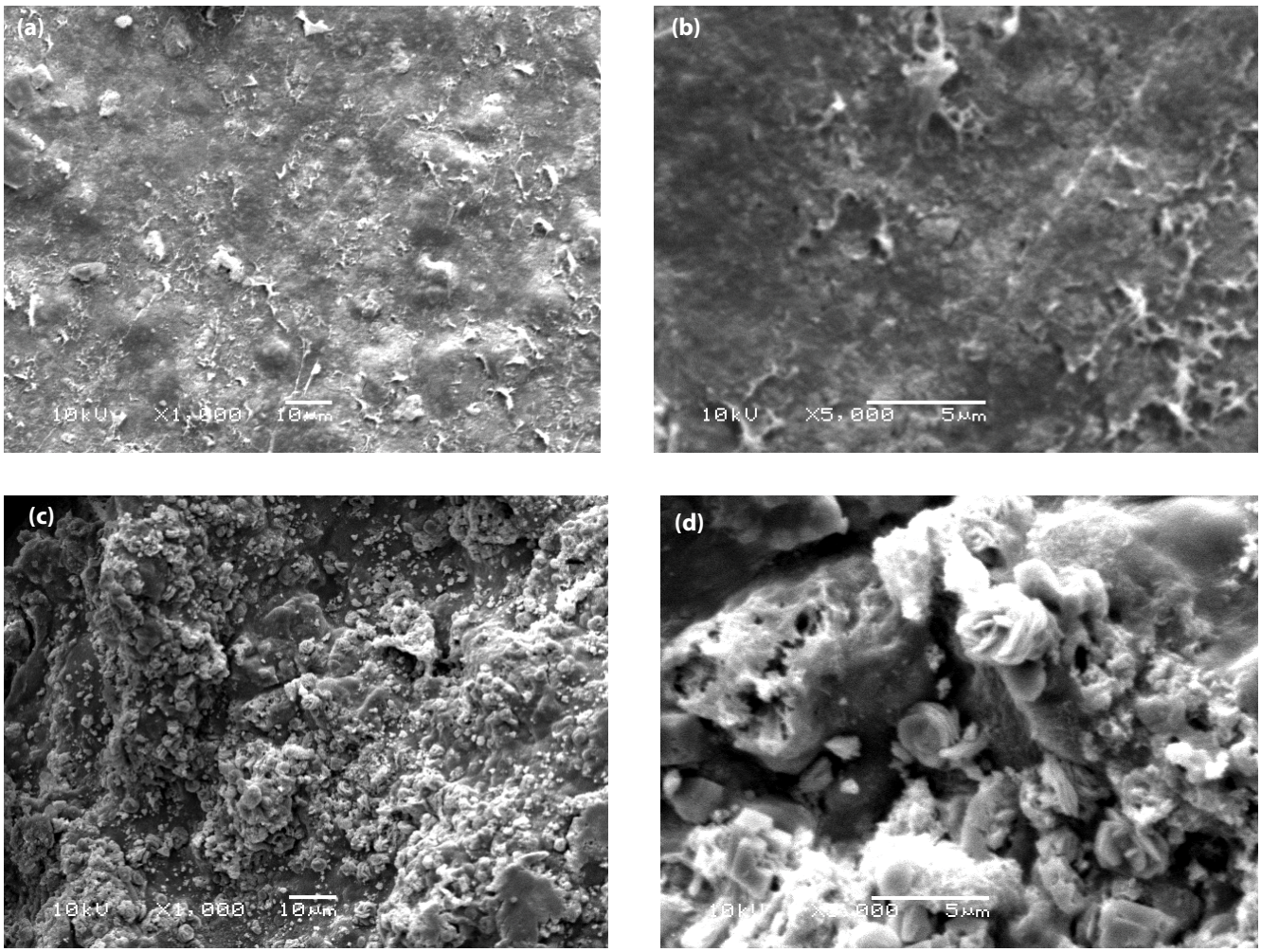

Fig. 5. SEM pictures of (a) Cs (Cs-1000X & (Cs-5000X)) and (b) Cs/MeB (Cs MeB-1000X & (Cs MeB-5000X)) hydrogels.

observations were extracted from Fig. 6. The first one is the fast removal of 80% MO only after 15 min using Cs/MeB hydrogel, while the chitosan hydrogel needs 75 min to achieve the same removal percentage. The second observation concerning the removal of almost 99% of MO dye molecules only after 45 min using Cs/MeB hydrogel and equilibrium reached. The equilibrium time reached after 120 min for chitosan hydrogel, where only 86% of MO dye molecules were removed. The superiority of the Cs/MeB hydrogel over its chitosan counterpart referred mainly to the newly formed porous structure as shown in Fig. 5b, and its direct impact on increasing the outer and pores internal surface area available for adsorption.

3.2.2. Effect of temperature

Fig. 7 demonstrates the impact of increased adsorption temperature from 25°C to 80°C on the MO dye removal (%) process using 25 mL of 5 ppm MO and 0.1 g adsorbent. The Figure shows two stages of the MO removal (%) for the chitosan adsorbent. The first stage was between 25°C and 40°C, where an exponential increment of the MO removal (%) from 47% to 86% were recognized. The second stage, beyond 40°C up to 80°C, shows a slow linear increment of the MO removal % from 86% to 91.5% at equilibrium. This behaviour disagrees with our previously published results [34], where a linear increment of the MO dye removal was observed. That disagreement may be referred to the higher concentration of GA used in this case (25%) compared with only 10% in the current work.

For Cs/MeB adsorbent, only one stage with a linear increment of the MO removal % from 80% to 97% at equilibrium has been observed in accordance with our previously published results removing MO dye by crosslinked chitosan derivate Schiff bases obtained from the coupling of chitosan with 1-vinyl 2-pyrrolidone Schiff base and 4-amino acetanilide Schiff base [34]. The Cs/MeB adsorbent shows an advantage over the chitosan adsorbent at room temperature, where the MO removal (%) of the Cs/MeB adsorbent (80%) is almost double of the chitosan adsorbent (47%). At a temperature higher than 40°C, The MO removal (%) for both adsorbents was found very close with a slight advantage of the Cs/MeB adsorbent.

An increase in temperature is known to increase the rate of diffusion of the adsorbate molecules across the external boundary layer and in the internal pores of the adsorbent

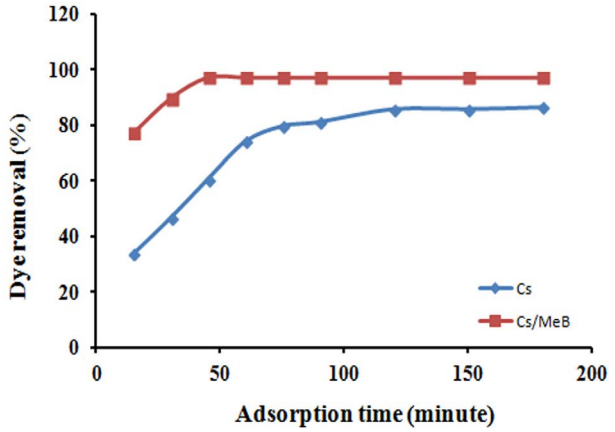

Fig. 6. Time profile of MO adsorption by Cs and Cs/MeB hydrogels.

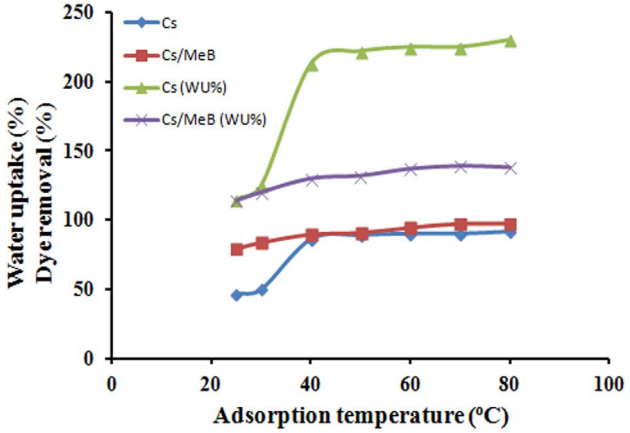

Fig. 7. Temperature profile of MO adsorption and water uptake (WU%) by Cs and Cs/MeB hydrogels.

particles as a result of the decreased viscosity of the solution [35]. Almeida et al. [36] suggested that a swelling effect within the internal structure of the adsorbent penetrating the large dye molecule is likely to occur when the temperature increases. In addition, Cestari et al. [37] reported that the dimensions of the chitosan pores increased with temperature. Our results agreed with the suggestion of Almeida et al. [36] and Cestari et al. [37], where the water uptake (%) of chitosan and Cs/MeB adsorbents is matched with the MO removal % behaviour.

3.2.3. Effect of pH

The effect of dye solution pH on the adsorption process was studied from 4 to 10 and presented in Fig. 8. Adsorption potency of MO as an anionic dye on chitosan is dependent on two factors, attractive force to the cationic charge of protonated amine groups and physical adsorption via van derval force and hydrophobic-hydrophobic interaction of methylene groups in acetyl groups and glucose ring. At pH 4.0, Cs/MeB displays the highest adsorption efficiency with removing per cent around 95% than Cs ~77%. Also, the cationic charges of Cs/MeB are lower than that of chitosan, but increase the surface area for adsorption via modification, as indicated in SEM photo (Fig. 5b), through pores formation, which provides an additional internal pores surface area from one side, and increase the outer surface area through new structures formed on the surface, flacks flowers like, from the other side. Also, the immobilization of the 4-methoxybenzyl molecules into the chitosan structure enhances the hydrophobic-hydrophobic physical adsorption between the benzene rings and the methyl hydrophobic groups. Linear decrement of the MO removal % by chitosan has been noticed due to continuous elimination of the cationic charge of chitosan amine groups from one side and collapse of the chitosan hydrogel structure with loss of its water content leading to reduce the surface are from the other side. The dye removal % declined linearly from 77% at pH 4 to about 3% at pH 10, where only the hydrophobic-hydrophobic physical adsorption is the dominant mechanism. On the other hand, the dye removal % by Cs/MeB was slightly affected by the increase of pH were decreased from 95% at pH 4.0 to 86% at pH 9.0. At the same time, a sharp decline of the dye removal % to 65% was observed at pH 10.0. This behaviour confirmed the dominated hydrophobic-hydrophobic physical adsorption between the benzene rings and the methyl hydrophobic groups of the Cs/MeB adsorbent and the MO dye molecules in a wide range of pH; from 4.0 to 9.0, while the elimination of the cationic charge of the last free amine groups at pH 10.0 leads to the collapse of the Cs/MeB hydrogel structure with loss of its water content leading to reduce the pores volume and so the internal pores surface area. The high and almost constant MO removal % by Cs/MeB hydrogel in a wide pH range is a great advantage for its application in the treatment of industrial effluents contaminated with MO dye.

3.2.4. Effect of Agitation

Different agitation rate varying from 50–250 rmp was applied to investigate its impact on the adsorption process of MO dye by Cs and Cs/MeB adsorbents. Fig. 9 shows two stages of MO dye removal behaviour for both adsorbents. The first stage observed between 50 and 150 rpm where almost a linear increase of the MO dye removal per cent from 35% to 69% for the chitosan adsorbent hydrogel while the Cs/MeB adsorbent shows a higher increase of the MO dye removal % from 25% to 86% within the same agitation speed range. Then, starts the second stage of the MO dye removal (%), with a much slower rate and approaching near equilibrium, between 150 and 250 rpm, where the chitosan adsorbent hydrogel removal % increases from 69% to 79% while the Cs/MeB adsorbent shows a similar behaviour where an increase of the MO dye removal % from 86% to 97% within the same agitation speed range.

In the process of dye adsorption initially, dye molecules have first to encounter the boundary layer effect, and then it has to spread from boundary layer film onto an adsorbent surface, which may explain the first stage between 50 rpm and 150 rpm range. Then finally, it has to distribute into the porous structure of the adsorbent, which may

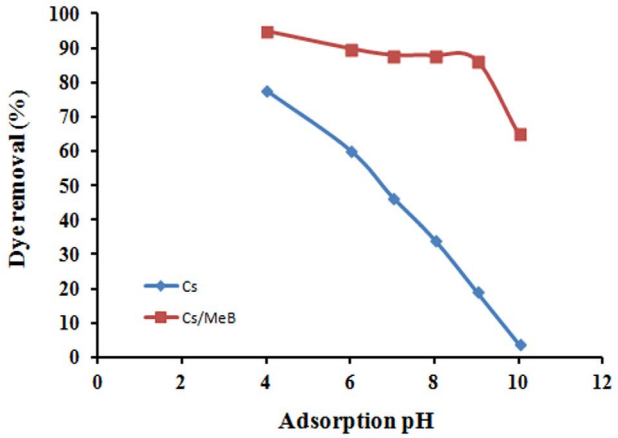

Fig. 8. pH profile of MO adsorption by Cs and Cs/MeB hydrogels.

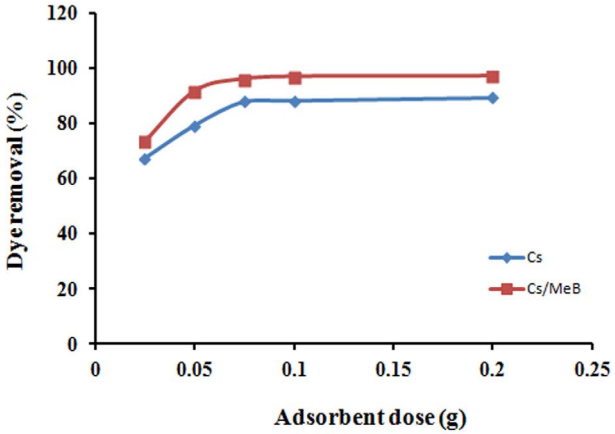

Fig. 10. Effect of adsorbent dose on MO adsorption by Cs and Cs/MeB hydrogels.

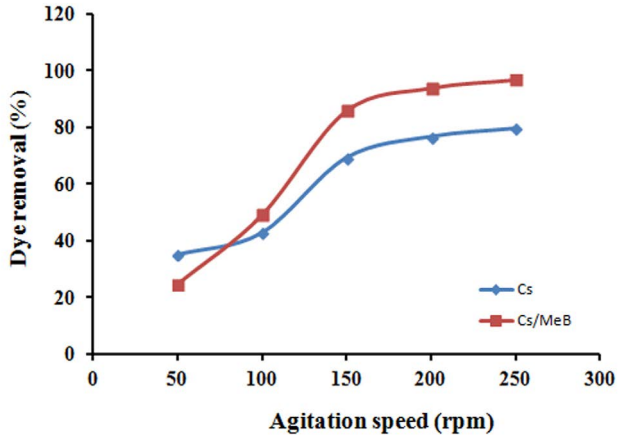

Fig. 9. Effect of agitation rate on MO adsorption by Cs and Cs/MeB hydrogels.

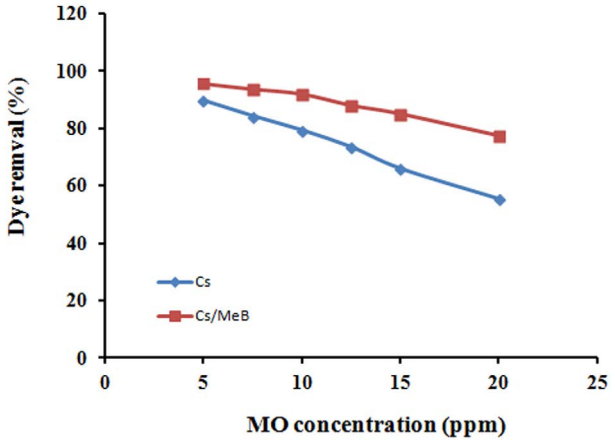

Fig. 11. Effect of MO concentration on adsorption percentages by Cs and Cs/MeB hydrogels.

explain the second stage between 150 and 250 rpm range [32]. The obtained behaviour is different from our previous results where almost a linear increment of the MO removal % was observed with the same agitation speed range, which was caused by the higher concentration of GA used in the crosslinking step in addition to the nature of the formed Schiff base [34].

3.2.5. Effect of adsorbent dose

The impact of hydrogel dose on MO removal was studied by changing the hydrogel content in the tested cell dye solution from 0.025 to 0.2 g at the same adsorption parameters. Fig. 10 shows increasing in removing per cent by the rise in the adsorbent dose that can be explained by the presence of extra active sites for dye adsorption [38,39]. It was also recognized that after a specific amount, the adsorption of the dye remains constant with a more addition in hydrogels, which indicated that the adsorption equilibrium reaches between adsorbent and adsorbate.

3.2.6. Effect of Methyl orange concentration

Fig. 11 shows the effect of initial MO concentration on the removing %. The removal percentage linearly reduced with an increase in initial MO concentration. This trend is due to the electrostatic repulsion between the dye molecules with increasing concentration that results in a competition between the dye molecules for the limited active sites in the adsorbent. A similar effect was observed with the other anionic dyes [39,40]. The obtained results are in accordance with the previously published result by the authors using chitosan derivate Schiff bases obtained from the coupling of chitosan with 1-vinyl 2-pyrrolidone and 4-amino acetanilide [34]. The maximum adsorption capacity for the chitosan and Cs/MeB at 20 ppm was found at 5.54 and 7.73 mg/g.

4. Conclusion

Novel crosslinked chitosan Schiff base derivate was developed by the coupling of chitosan with 4-methoxybenzaldehyde to have chitosan Schiff base (Cs/MeB) for the

adsorption of anionic reactive dye (Methyl orange) from aqueous solutions. The results showed a very fast adsorption rate of the MO by the chitosan Schiff base derivate, where the equilibrium was attained after only 45 min compared with 120 min for chitosan. Variation of the initial dye concentration reduced the removal percentage at a linear mode using fixed adsorbent dosage. Within the studied range of MO concentration, the developed chitosan Schiff base hydrogel shows a constant adsorption ability over wide ranges of temperature (40°C–80°C) and pH (4.0–9.0) for the Cs/MeB Schiff base of the wastewater. The obtained behaviour nominates the developed chitosan Schiff base hydrogel to work under a wide range of operational conditions.

References

[1] D. Musmarra, M. Prisciandaro, M. Capocelli, D. Karatza, P. Iovino, S. Canzano, A. Lancia, Degradation of ibuprofen by hydrodynamic cavitation: reaction pathways and effect of operational parameters, Ultrason. Sonochem., 29 (2016) 76–83.

[2] S. Sarode, P. Upadhyay, M.A. Khosa, T. Mak, A. Shakir, S. Song, A. Ullah, Overview of wastewater treatment methods with special focus on biopolymer chitin-chitosan, Int. J. Biol. Macromol., 121 (2019) 1086–1100.

[3] L. Rizzo, S. Malato, D. Antakyali, V.G. Beretsou, M.B. Đolić, W. Gernjak, E. Heath, I. Ivancev-Tumbas, P. Karaolia, A.R. Lado Ribeiro, G. Mascolo, C.S. McArdell, H. Schaar, A.M.T. Silva, D. Fatta-Kassinos, Consolidated vs new advanced treatment methods for the removal of contaminants of emerging concern from urban wastewater, Sci. Total Environ., 655 (2019) 986–1008.

[4] M.T. Yagub, T.K. Sen, S. Afroze, H.M. Ang, Dye and its removal from aqueous solution by adsorption: a review, Adv. Colloid Interface Sci., 209 (2014) 172–184.

[5] A. Srinivasan, T. Viraraghavan, Decolorization of dye wastewaters by biosorbents: a review, J. Environ. Manage., 91 (2010) 1915–1929.

[6] A. Mittal, A. Malviya, D. Kaur, J. Mittal, L. Kurup, Studies on the adsorption kinetics and isotherms for the removal and recovery of Methyl orange from wastewaters using waste materials, J. Hazard. Mater., 148 (2007) 229–240.

[7] F. Gulshan, S. Yanagida, Y. Kameshima, T. Isobe, A. Nakajima, K. Okada, Various factors affecting photodecomposition of methylene blue by iron-oxides in an oxalate solution, Water Res., 44 (2010) 2876–2884.

[8] E. Alventosa-de Lara, S. Barredo-Damas, M.I. Alcaina-Miranda, M.I. Iborra-Clar, Ultrafiltration technology with a ceramic membrane for reactive dye removal: optimization of membrane performance, J. Hazard. Mater., 209–210 (2012) 492–500.

[9] S. Raghu, C.W. Lee, S. Chellammal, S. Palanichamy, C.A. Basha, Evaluation of electrochemical oxidation techniques for degradation of dye effluents-a comparative approach, J. Hazard. Mater., 171 (2009) 748–754.

[10] F.P. Van der Zee, S. Villaverde, Combined anaerobic-aerobic treatment of azo dyes-a short review of bioreactor studies, Water Res., 39 (2005) 1425–1440.

[11] N. Mohammadi, H. Khani, V.K. Gupta, E. Amereh, S. Agarwal, Adsorption process of Methyl orange dye onto mesoporous carbon material-kinetic and thermodynamic studies, J. Colloid Interface Sci., 362 (2011) 457–462.

[12] R.S. Dassanayake, S. Acharya, N. Abidi, Recent advances in biopolymer-based dye removal technologies, Molecules 26 (2021) 4697, doi: 10.3390/molecules26154697.

[13] G.Z. Kyzas, D.N. Bikiaris, A.C. Mitropoulos, Chitosan adsorbents for dye removal: a review, Polym. Int., 66 (2017) 1800–1811.

[14] T.M. Freire, L.M.U.D. Fechine, D.C. Queiroz, R.M. Freire, J.C. Denardin, N.M.P.S. Ricardo, T.N.B. Rodrigues, D.R. Gondim, I.J.S. Junior, P.B.A. Fechine, Magnetic porous controlled Fe_3O_4–chitosan nanostructure: an eco-friendly adsorbent for efficient removal of azo dyes, Nanomaterials, 10 (2020) 1194, doi: 10.3390/nano10061194.

[15] L. Dong, C. Wen, Y. Junxia, D. Yigang, Polyamine chitosan adsorbent for the enhanced adsorption of anionic dyes from water, J. Dispersion Sci. Technol., 38 (2017) 1832–1841.

[16] A. Labidi, A.M. Salaberria, S.C.M. Fernandes, J. Labidi, M. Abderrabba, Functional chitosan derivative and chitin as decolorization materials for Methylene blue and Methyl orange from aqueous solution, Materials, 12 (2019) 361, doi: 10.3390/ma12030361.

[17] M.N. Ahmad, A. Hussain, M.N. Anjum, T. Hussain, A. Mujahid, M.H. Khan, T. Ahmed, Synthesis and characterization of a novel chitosan-grafted polyorthoethylaniline biocomposite and utilization for dye removal from water, Open Chem., 18 (2020) 843–849.

[18] E.A. Alabbad, Efficient removal of Methyl orange from wastewater by polymeric chitosan-iso-vanillin, Open Chem. J., 7 (2020) 16–25.

[19] G. Yuvaraja, D-Y. Chen, J.L. Pathak, J. Long, M.V. Subbaiah, J.-C. Wen, C.-L. Pan, Preparation of novel aminated chitosan Schiff's base derivative for the removal of Methyl orange dye from aqueous environment and its biological applications, Int. J. Biol. Macromol., 146 (2020) 1100–1110.

[20] C. Huang, H. Liao, X. Ma, M. Xiao, X. Liu, S. Gong, X. Shu, X. Zhou, Adsorption performance of chitosan Schiff base towards anionic dyes: electrostatic interaction effects, Chem. Phys. Lett., 780 (2021) 138958, doi: 10.1016/j.cplett.2021.138958.

[21] E.A. Soliman, S.M. El-Kousy, H.M. Abd-Elbary, A.R. Abou-zeid, Low molecular weight chitosan-based Schiff bases: synthesis, characterization and antimicrobial activity, J. Food Technol., 8 (2013) 17–30.

[22] Y.N. Dai, P. Li, J.P. Zhang, A.Q. Wang, Q. Wei, Swelling characteristics and drug delivery properties of nifedipine-loaded pH sensitive alginate–chitosan hydrogel beads, J. Biomed. Mater. Res. Part B, 86B (2008) 493–500.

[23] S.P. Ramnani, S. Sabharwal, Adsorption behavior of Cr(VI) onto radiation crosslinked chitosan and its possible application for the treatment of wastewater containing Cr(VI), React. Funct. Polym., 66 (2006) 902–909.

[24] G. Palma, P. Casals, G. Cardena, Synthesis and characterization of new chitosan-o-ethyl phosphonate, J. Chil. Chem. Soc., 50 (2005) 719–724.

[25] T.M. Tamer, M.A. Hassan, A.M. Omer, W.M.A. Baset, M.E. Hassan, M.E.A. El-Shafeey, M.S. Mohy Eldin, Synthesis, characterization and antimicrobial evaluation of two aromatic chitosan Schiff base derivatives, Process Biochem., 51 (2016) 1721–1730.

[26] T.M. Tamer, M.A. Hassan, A.M. Omer, K. Valachová, M.S. Mohy Eldin, M.N. Collins, L. Šoltés, Antibacterial and antioxidative activity of O-amine functionalized chitosan, Carbohydr. Polym., 169 (2017) 441–450.

[27] A. Pawlak, M. Mucha, Thermogravimetric and FTIR studies of chitosan blends, Thermochim. Acta, 396 (2003) 153–166.

[28] F.A.A. Tirkistani, Thermal analysis of some chitosan Schiff bases, Polym. Degrad. Stab., 60 (1998) 67–70.

[29] M.K. Cheung, K.P.Y. Wan, P.H. Yu, Miscibility and morphology of chiral semicrystalline poly-(R)-(3-hydroxybutyrate)/chitosan and poly-(R)-(3-hydroxybutyrate-co-3-hydroxyvalerate)/chitosan blends studied with DSC, 1H T1 and$T1_\rho$ CRAMPS, J. Appl. Polym. Sci., 86 (2002) 1253–1258.

[30] V. Gonzalez, C. Guerrero, U. Ortiz, Chemical structure and compatibility of polyamide–chitin and chitosan blends, J. Appl. Polym. Sci., 78 (2000) 850–857.

[31] F.S. Kittur, H. Prashanth, K.U. Sankar, R.N. Tharanathan, Characterization of chitin, chitosan and their carboxymethyl derivatives by differential scanning calorimetry, Carbohydr. Polym., 49 (2002) 185–193.

[32] M. Shanker, T. Chinniagounder, Adsorption of reactive dye using low cost adsorbent: cocoa (*Theobroma cacao*) Shell, World Appl. Environ. Chem., 1 (2012) 22–29.

[33] A. El Nemr, O. Abdelwahab, A. El-Sikaily, A. Khaled, Removal of Direct blue-86 from aqueous solution by new activated

carbon developed from orange peel, J. Hazard. Mater., 161 (2009) 102–110.
[34] E.M. El-Sayed, T.M. Tamer, A.M. Omer, M.S. Mohy Eldin, Development of novel chitosan Schiff base derivatives for cationic dye removal: Methyl orange model, Desal. Water Treat., 57 (2016) 22632–22645.
[35] Z. Al-Qodah, Adsorption of dyes using shale oil ash, Water Res., 34 (2000) 4295–4303.
[36] C.A.P. Almeida, N.A. Debacher, A.J. Downs, L. Cottet, C.A.D. Mello, Removal of methylene blue from colored effluents by adsorption on montmorillonite clay, J. Colloid Interface Sci., 332 (2009) 46–53.
[37] A.R. Cestari, E.F.S. Vieira, A.A. Pinto, E.C.N. Lopes, Multiple adsorption of anionic dyes on silica/chitosan hybrid 1. Comparative kinetic data from liquid- and solid-phase models, J. Colloid Interface Sci., 292 (2005) 363–372.
[38] H. Hou, R. Zhou, P. Wu, L. Wu, Removal of Congo red dye from aqueous solution with hydroxyapatite/chitosan composite, Chem. Eng. J., 211–212 (2012) 336–342.
[39] A. Szyguła, E. Guibal, M.A. Palacın, M. Ruiz, A.M. Sastre, Removal of an anionic dye (Acid blue 92) by coagulation-flocculation using chitosan, J. Environ. Manage., 90 (2009) 2979–2986.
[40] M.S. Chiou, H.O. Pang-Yen, H.-Y. Li, adsorption of anionic dyes in acid solutions using chemically crosslinked chitosan beads, Dyes Pigm., 60 (2004) 69–84.